Performance Improvement in the Design of Broad-Beam Microstrip Reflectarray

Piyaporn Krachodnok and Rangsan Wongsan

***Abstract*— This is a theoretical and experimental study of microstrip reflectarray useable in wireless local area networks (WLAN). The effectiveness of reducing the unit cell size of microstrip reflectarray which is duplicated the same radiating aperture as quadratic backscatter was investigated. A reflectarray with variable element sizes and reduced grid spacing have been designed at 10 GHz. For a given number of elements, it is shown that increased gain can be attainted for reduced unit cell size with no significant change in array size. To confirm the validity of this approach, an X-band antenna prototype was designed and developed. It was experimentally tested and showed good performance characteristics.**

***Index Terms*— reflectarray, broad-beam antenna**

I. Introduction

A planar reflector or microstrip reflectarray is a printed low-profile antenna that consists of a grounded flat onto which a quasi-periodic array of resonant conducting element (patches or dipoles) is etched [1]-[4]. This operation is similar in concept to a parabolic reflector that naturally forms a planar phase front when a feed is placed at its focus. Each element phase can be adjusted to produce a required phase law over the antenna aperture.

In the wireless communication applications such as wireless local area network (WLAN) large-scale indoor base station [5], it is desirable the antenna which has wide beam to cover a broad area. In principle, we have an antenna which is installed on the center point of ceiling in the very large room and can illuminate a predefined area for all users without substantial spatial variation. Consequently, the all client computers, which are in this room, will be connected to the access point of WLAN through the only one antenna. The wide beam reflectarray for WLAN antenna is an alternative as shown in Fig. 1 [6]. A reflectarray configuration is attractive because it allows a single mechanical design to be used repeatedly for a wide variety of different coverage specifications. The only changes are required that the printed reflecting element dimensions can be changed for each design, in order to generate the new shaped beam. Thus, many of the high recurring costs associated with shaped-reflector antennas can be eliminated with flat printed reflectarrays [7]. The flat geometry of a reflectarray also lends itself to easier placement and deployment on the WLAN large-scale indoor base station and also in terms of manufacture.

However, it is generally observed that when the antenna beam is enlarged, the antenna gain is reduced. In this paper, we have investigated the influence of the unit cell size of reflectarray on the gain performance. To achieve such broad-beamwidth, phase of each array element in the reflectarray antenna is designed specifically to emulate the curvature of the backscatter function by using patches of different sizes. As the patch shape is not the aim of this work, it has been chosen to be simple to design regarding to the element position variation.

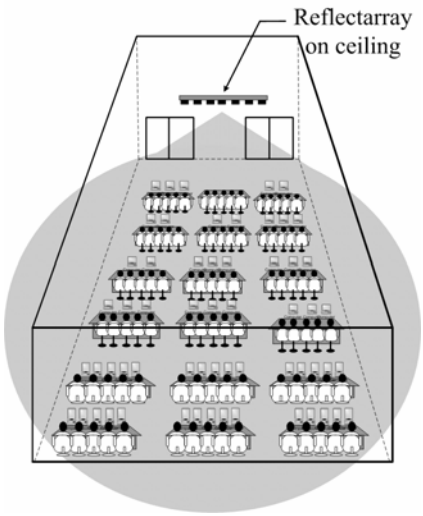

Figure 1. Reflectarray for WLAN large-scale indoor base station.

The first section, we will present the design approach as far as it concerns the unit cell size determination (Section II) and the reflection phase characteristic (Section III). In section IV, we apply this approach to calculate the radiation pattern of the proposed antenna. The reflectarray using quadratic backscatter function was then tested experimentally in section V. An antenna, fabricated according to the theoretical model, was made and tested in-house. Finally, the conclusions are given in section VI.

Manuscript received October 30, 2007. This work was supported in part by the Research Department, Institute of Engineering, Suranaree University of Technology, THAILAND.

P. K. and R. W are with the School of Telecommunication Engineering, Institute of Engineering, Suranaree University of Technology, Muang, Nakhon Ratchasima 30000, THAILAND. (corresponding author to provide phone: +66-44224392; fax: +66-44224603, e-mail: priam@ sut.ac.th).

II. Unit Cell Size Determination

Fig. 2 illustrates the geometry of an infinite reflectarray element. As indicated, *s* is the center-to-center elements spacing in both *x* and *y* directions that its size equal to unit cell size and *L* is the element size. To avoid the physical contacts among the adjacent elements, the unit cell size is must be larger than the element size *L*,

$$\min\{\text{unit cell size}\} = L. \tag{1}$$

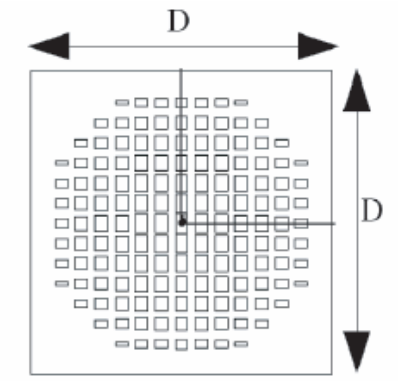

(a)

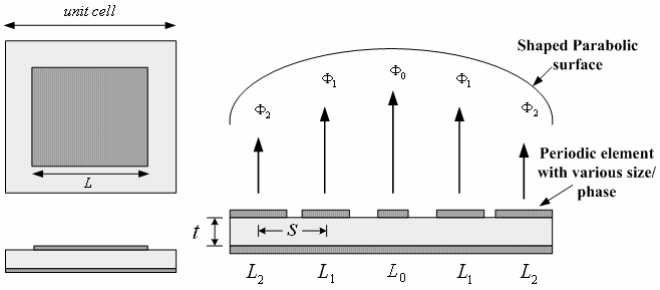

(b)

Figure 2. Geometry of an infinite reflectarray element.

The effective method for decreasing the unit cell size is to print the element on substrate, which reduces the size of reflectarray element. In microstrip antenna, many techniques have been reported to reduce the size of reflectarray element at a fixed operating frequency [8]. In general, reflectarray elements are half-wavelength structures at reflection phase 180° and operated at a resonant frequency, which is given by

$$f_0 \cong \frac{c}{2L\sqrt{\varepsilon_r}}, \tag{2}$$

where *c* is the speed of light and ε_r is the relative permittivity of the grounded microwave substrate. From (2), it is found that the physical unit cell size of reflectarray will be decreased at a fixed operating frequency due to the use of the microwave substrate with a larger permittivity.

III. Reflection Phase Characteristic

A. Backscatter Function for Broad-Beam Reflectarray

In Fig. 2 (a), the perspective upper side view of the proposed antenna which is duplicated the same radiating aperture as quadratic backscatter fed by standard X-band horn. Fig. 3 shows the quadratic distribution of backscatter curvature by using the geometrical function as expressed in (3). Where *D* is assumed to be the diameter and *A* is the depth of the quadratic backscatter reflector, respectively. With a given feed horn as shown in Fig. 4, the appropriate distance between the horn and the center of reflectarray can be estimated by considering the spillover and taper efficiencies relations given in [9],[10]. At optimum value of aperture efficiency, a feed distance to diameter ratio (*f/D*) provides spillover and taper efficiencies of 76% and 84% respectively. Thus feed distance is chosen to be of 21.25 cm at 10λ reflector diameter. This structure radiates the beam that illuminates a predefined circular area without substantial spatial variation.

$$f(z') = A(1-(\frac{2}{D}z')^2); \quad -\frac{D}{2} \le z' \le \frac{D}{2} \tag{3}$$

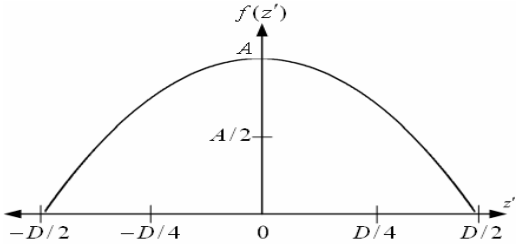

Figure 3. Quadratic distribution.

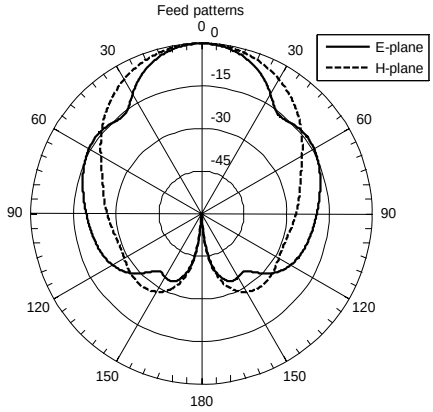

Figure 4. Radiation pattern of standard X-band Horn.

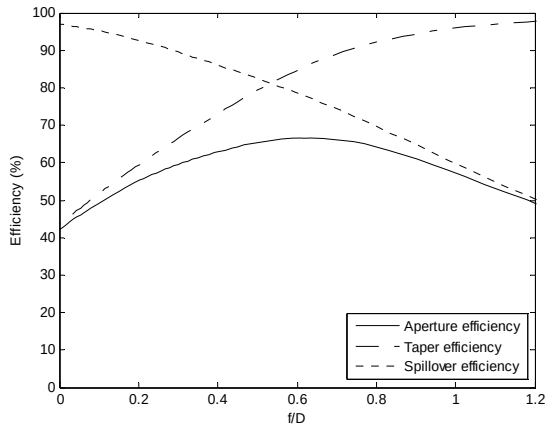

Figure 5. Aperture efficiency of reflectarray.

B. Required Phase Delay

Fig. 6 depicts the analysis model of broad-beam microstrip reflectarray [6], which parameters used in this figure are described below:

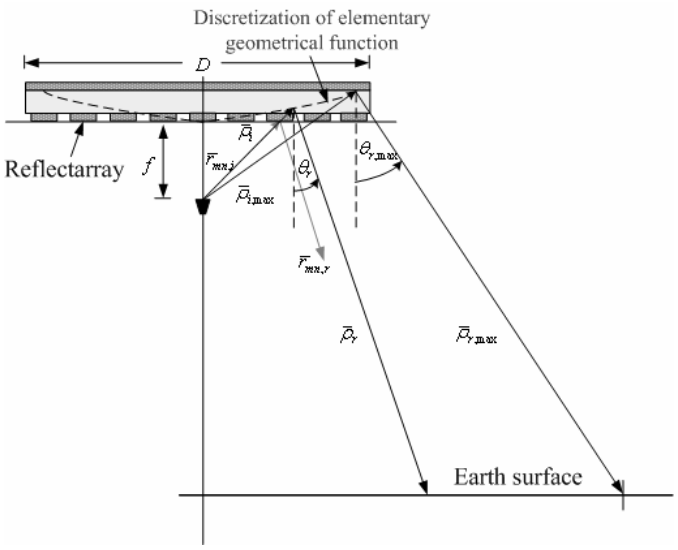

Figure 6. Analysis model of broad-beam microstrip reflectarray.

$\vec{r}_{mn,i}$ the vector from the feed to the *mn*-th reflectarray element, which can be obtained by using flat geometry;

$\vec{r}_{mn,r}$ the reflected vector from the reflectarray surface to far-field;

$\vec{\rho}_i$ the vector from the feed to the shaped reflector surface, which can be obtained by using curvature geometry;

$\vec{\rho}_r$ the reflected vector from the shaped reflector surface to far-field;

θ_i incidence angle;

θ_r reflection angle;

D diameter of the reflector;

f distance between the feed and the center of the reflectarray.

In general, the feed may be positioned at distance from the reflectarray. The path lengths from the feed to all reflectarray elements are all different, which lead to different phase delays. The required phase, which is induced on the array, has to compensate for phase delay, $\Delta\Phi_{mn}$, between patch elements and surface of quadratic backscatter as given by (4).

$$\Delta\Phi_{mn} \text{ in degree} = \left[(1-N)k_0 \left(|\vec{\rho}_i| + \frac{z_b - f}{\sin\theta_r} - |\vec{r}_{mn,i}| \right) \right] \frac{360}{2\pi}, \qquad (4)$$

where (x_b, y_b, z_b) describes the coordinate of the quadratic backscatter function and N is integer. From (4) indicates that the compensating phase can be repeated every 360 degree and the portion that is an integer multiple of 360 degree can be deleted.

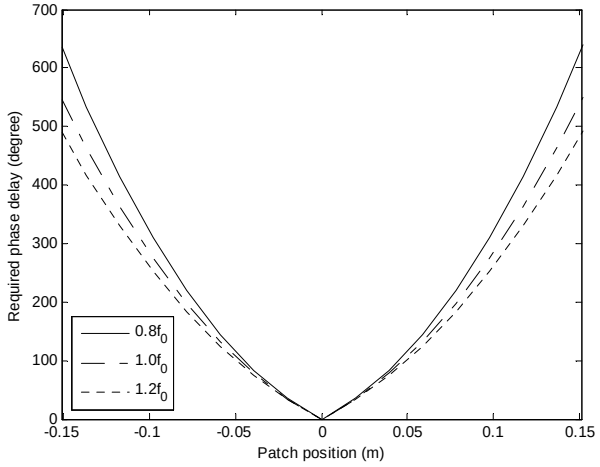

Figure 7. Calculated results of desired reflection phase properties.

The required phase delay that related to the patch position is determined for shaping beam of reflectarray as shown in Fig. 7 with various center frequencies (f_0 = 10 GHz). These phases are duplicated the same radiating aperture as shape of quadratic backscatter. In the design, the cell elements are printed on a TACONIC substrate with thickness 0.762 mm and permittivity ε_r = 2.33 and 6.15, respectively. Because reduction of center-to-center element spacing changes the elements position, the phase delays are decreased.

C. Element Characterization

The most important and critical segment of the reflectarray design is its element characterization. To compensate for above phase delays, the elements must have corresponding phase advancements designed. Its phase change versus element change (patch size, etc.) must be calibrated correctly. If the

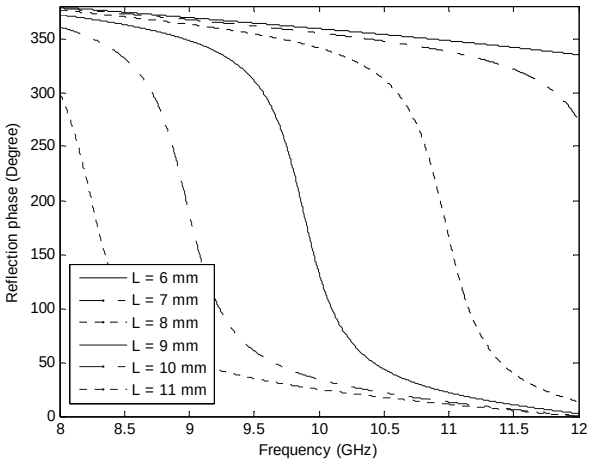

(a)

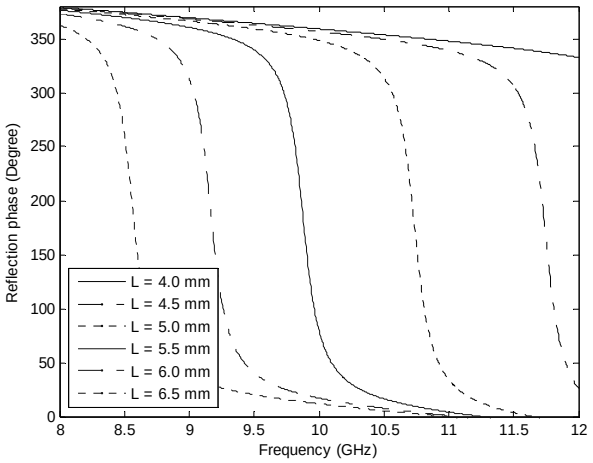

(b)

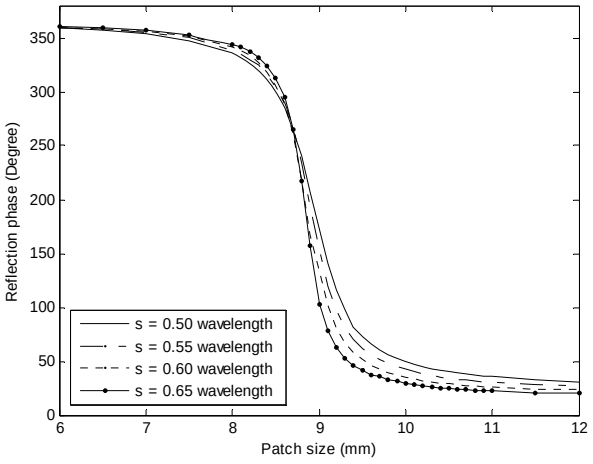

(c)

Figure 8. Simulated results of element characterization: (a) at ε_r = 2.33, s = 0.6 λ_0, (b) at ε_r = 6.15, s = 0.6 λ_0, (c) at ε_r = 2.33, f_0 = 10 GHz.

element design is not optimized, it will not scatter the signal from the feed effectively to form an efficient far-field beam. In this paper, the phase calibration technique is to use a full-wave method of moment and the infinite-array approach [6],[10] to model the effect of the finite grounded dielectric substrate underlying the single radiator.

Fig. 8 shows simulated results of reflection phase of infinite array. The obtained results indicated that, if the element size L is excessively small, either the reflection phase cannot be made to cover the full required 0° to 360° phase range, or it changes excessively fast around the element resonance. This available phase shift rang is limited by the reflectarray antenna bandwidth (around 4%). In Fig. 8(c), the reductions of unit cell size of reflectarray can reduce the slope of the phase response. For achieving reflectarray element with a reduced size at a fixed operating frequency, the use of a high-permittivity substrate is an effective method as shown in Fig. 8 (a)-(b).

IV. Calculation of Radiation Pattern

With the compensating phases of all elements known, the far-field radiation patterns can be calculated by the conventional array theory [9], where the radiations of all elements are summed together as follows. Considering a planar array consisting of $M \times N$ elements that are nonuniformly illuminated by a low-gain feed, the reradiated field from the patches in an arbitrary direction, $\hat{u}$, will be of the form,

$$E(\hat{u}) = \sum_{m=1}^{M}\sum_{n=1}^{N} F(\vec{r}_{mn}\cdot\hat{a}_z)\cdot A(\vec{r}_i\cdot\hat{u}_r)\cdot A(\hat{u}\cdot\hat{u}_r) \cdot \exp\left[-jk_0\left(|\vec{r}_{mn}|+\vec{r}_i\cdot\hat{u}\right)-j\Delta\Phi_{mn}\right], \tag{5}$$

where F is the feed pattern function, A is the reflectarray element pattern function, $\vec{r}_i$ is the vector from the centre of reflectarray to *mn*-th element. $\hat{u}_r$ is the reflected field pointing direction, and $\Delta\Phi_{mn}$ is the required compensating phase of the *mn*-th element calculated by (4).

Table I
Characteristics of reflectarray.

Unit cell size (wavelength)	HPBW (degree)	Maximum Gain (dBi)
0.3	122	22.61
0.4	126	19.27
0.5	142	15.54
0.6	146	11.88
0.7	152	11.33

The radiated field from (5) provides the radiation characteristics, which are represented in Table I and Fig. 9 for various unit cell sizes. The primary feed used in the design is a standard X-band horn, which is placed along the H-plane at a focus f = 21.25 cm. The prescribed field requirements have been satisfied by an appropriate choice of the radiating patches selected from the complex design curves obtained in the analysis stage. The steepness of the pattern edges and the angular positions of these edges confirm that the antenna efficiently illuminates the target area to be covered (±65°). Because of phase change versus element change, each unit cell size provides different characteristics such as -3 dB beam width (HPBW) and gain performance. The maximum gain is increased due to reduction of grid spacing. Thus, the HPBW is decreased and followed by the same order as the maximum gain. Fig. 10 shows maximum gain and gain at elevation angle 0° with various unit cell sizes.

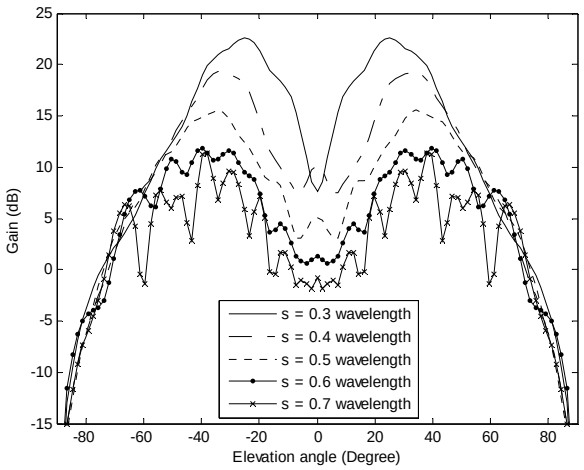

Figure 9. Radiation pattern of quadratic function.

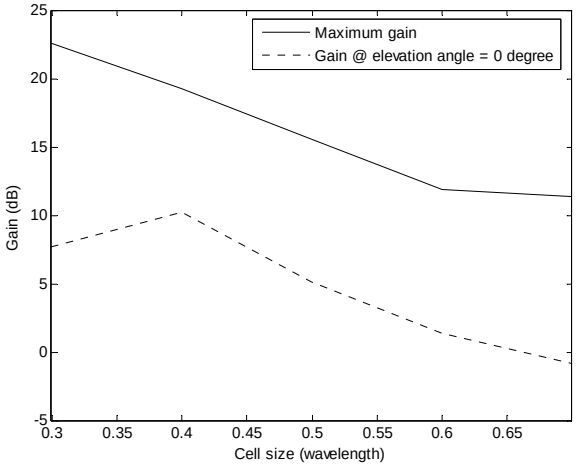

Figure 10. Gain versus unit cell size.

V. Experimental Results

To verify the theoretical calculation, the experiment was set up at the operating frequency of 10 GHz. This frequency was chosen to best utilize the available equipment. The prototype antenna was fabricated and is shown photographed in Fig. 11. The aperture shape of a reflectarray is a 30 cm by 30 cm. Figs. 11(b) and (c) show the upper side of the reflectarrays. Patch size is optimized by numerical simulations provided by the tool in section III (C). As can be seen each element on the antenna has varying size in order to provide the desired field pattern. We have investigated and compared measured performances of reflectarrays with $0.3\lambda_0$ and $0.6\lambda_0$ unit cell sizes, respectively. The substrate is TACONIC of 0.762mm thickness and dielectric constant 2.33 for $s = 0.6\lambda_0$ and 6.15 for $s = 0.3\lambda_0$, respectively. Phase range compensations shown in Fig.12 are of 348° for the $0.6\lambda_0$ unit cell size and 325° for the $0.3\lambda_0$ one.

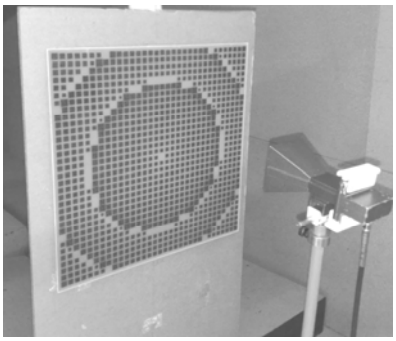

(a)

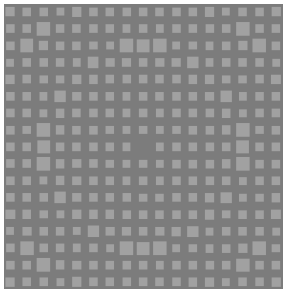

(b) $s = 0.6\ \lambda_0$, 17×17 elements

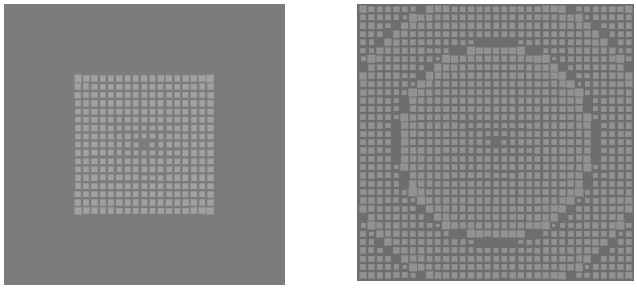

17×17 elements 33×33 elements

(c) $s = 0.3\ \lambda_0$

Figure 11. Photograph of the reflectarray antenna with various unit cell sizes and array sizes.

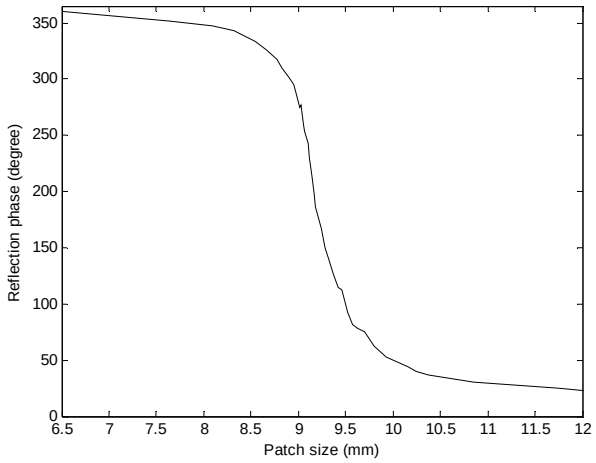

(a)

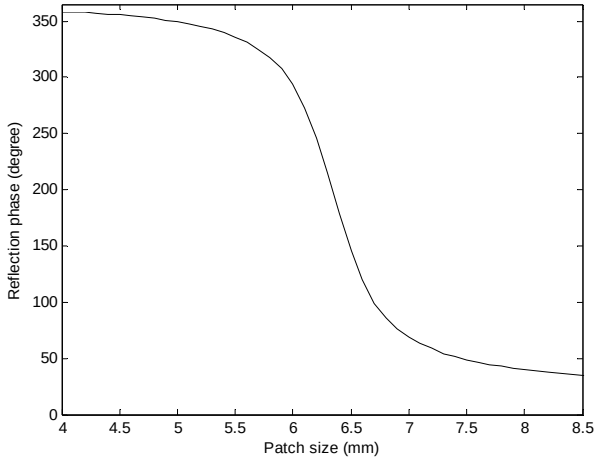

(b)

Figure 12. Reflection coefficient phase versus patch size (L): (a) at $s = 0.6\ \lambda_0$, (b) at $s = 0.3\ \lambda_0$.

The radiation patterns were measured in an anechoic chamber using vector network analyzer HP 8722D and standard X-band horn. The measurement set up comprises two antennas, faced together at far field distance ($R > 2D^2 / \lambda$). The measured far-field patterns in H- and E-planes for the test antenna at the resonant frequency of 10 GHz are illustrated in Figs. 13 and 14. These figure show the comparison with the respective theoretical patterns computed as the superimposition of the fields radiated by the array elements when the correct incidence angles are considered. Because of the feed blocking effect and the coupling between primary the source and the reflectarray by simulation are neglected, therefore, the dip in pattern boresight from measurement of around 4 dB are occurred. Nevertheless, we found that the ripple appears on the envelope of measured patterns, which are caused from some multipath effect that provided by construction of feed horn and metallic masts. Furthermore, if we compare the average levels on the all curves of each plane in far angle region, it will be observed that a difference from measured pattern on the order of 2 dB approximately for numerical result. However, the agreement between simulated and measured results is satisfactory.

On this 17×17 reflectarray element with different element dimensions are fixed. We consider the effect on unit cell size reduction with the same aperture dimension. Due to the small size of the array elements, the number of rings with missing phase values is only of one. Thus their effect is decreased. From the measurement reported in Table II, the verification between simulation and experiment has been presented in the parameters of maximum gain and HPBW. It is obvious that the effect on the broad-beam pattern improvement is the same as the simulated results. The improvement of maximal gain is of about 9 dB for the reduction of unit cell size from $0.6\lambda_0$ to $0.3\lambda_0$. The maximum gain of simulated results by using $0.6\lambda_0$ unit cell size in E-plane and H-plane patterns are higher than measured results around 0.05 dB and 0.81 dB, respectively, while the maximum gain of simulation by using $0.3\lambda_0$ unit cell size are higher than measured results around 1.14 dB and 0.94 dB, respectively. Besides that the measured results of HPBW are wider than the simulated results around 5º in E-plane and 13º in H-plane for $0.6\lambda_0$ unit cell size and around 21º in E-plane and 12º in H-plane for $0.3\lambda_0$ unit cell size. Therefore, it can be summarized that the maximum gain and HPBW between simulated and measured results can show some minor differences both in E-plane and H-plane pattern.

The larger array size of 33×33 elements ($s = 0.3\lambda_0$) have been made and tested to improve performance. The number of uncorrected rings increases in comparison to the smaller array size as shown in Fig. 11(c). The results are plotted in Fig. 14. It is obvious that the formerly HPBW improvements when the array size is larger at fixed aperture dimension. The gain increases of about 2 dB.

Table II
Comparison of simulated and measured results for antenna characteristics

Antenna characteristics	Simulated		Measured	
	E-plane	H-plane	E-plane	H-plane
Maximum Gain (dBi)				
$s = 0.6\lambda_0$, 17×17 elements	8.49	10.65	8.44	9.84
$s = 0.3\lambda_0$, 17×17 elements	19.04	19.94	17.9	19
$s = 0.3\lambda_0$, 33×33 elements	18.62	20	19.14	20.54
HPBW (degree)				
$s = 0.6\lambda_0$, 17×17 elements	137	151	132	164
$s = 0.3\lambda_0$, 17×17 elements	105	112	84	100
$s = 0.3\lambda_0$, 33×33 elements	108	125	116	120

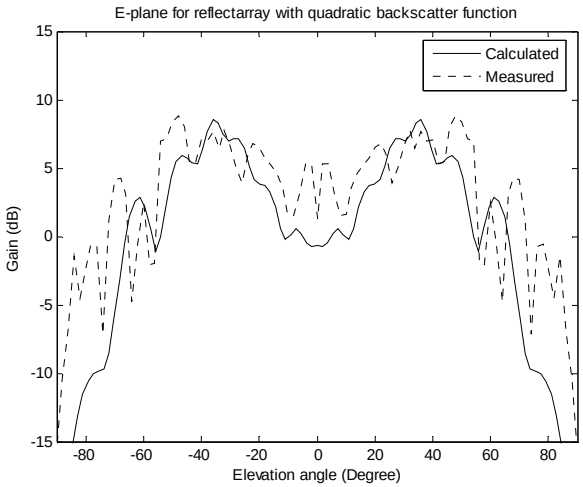

(a) E-plane at $s = 0.6\ \lambda_0$

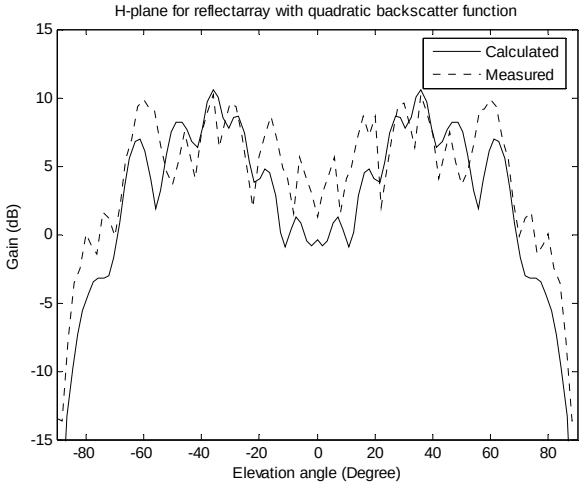

(b) H-plane at $s = 0.6\ \lambda_0$

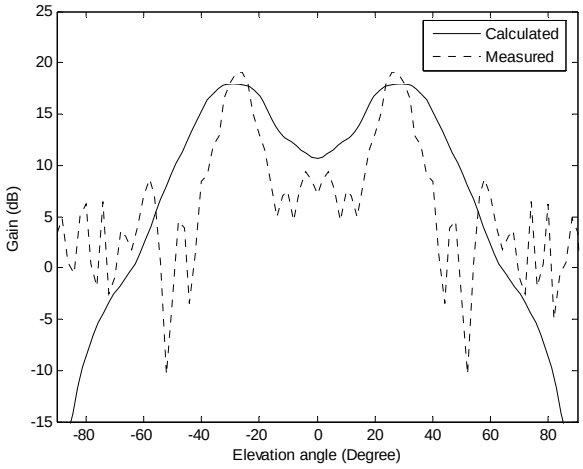

(c) E-plane at $s = 0.3\ \lambda_0$

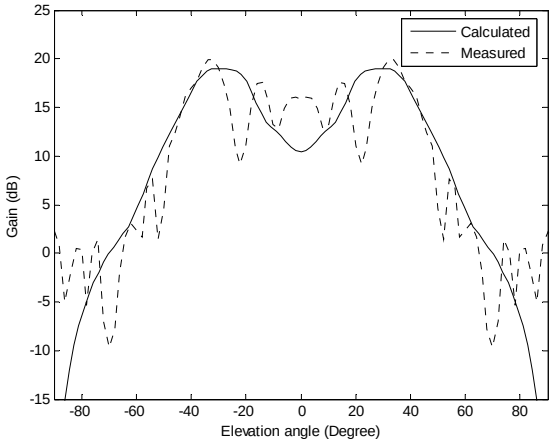

(d) H-plane at $s = 0.3\ \lambda_0$

Figure 13. Measured and calculation gain patterns of the proposed antenna with 17×17 elements

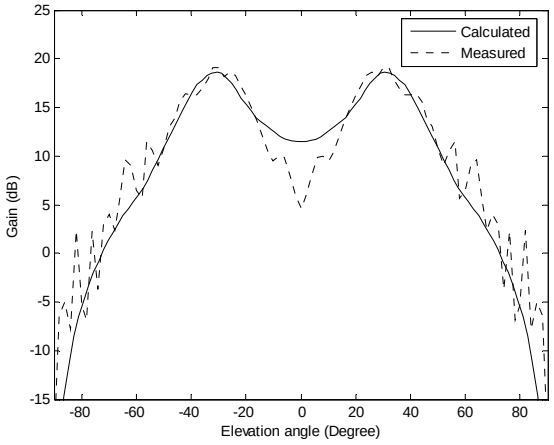

(a) E-plane at $s = 0.3\ \lambda_0$

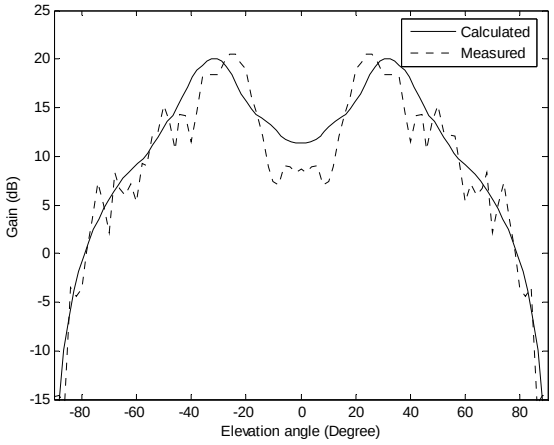

(b) H-plane at $s = 0.3\ \lambda_0$

Figure 14. Measured and calculation gain patterns of the proposed antenna with 33×33 elements

VI. Conclusion

A broad-beam microstrip reflectarray designed from square patch has been presented. The prescribed field requirements have been satisfied by an appropriate choice of the radiating patches array selected from the complex design curves obtained in the analysis stage. Simulation of this reflectarray demonstrates that reduction of unit cell size can enhance bandwidth or reduce the slope of the reflection phase. In addition, the maximum gain is improved with small significant change in HPBW. A test antenna built according to our model is in good agreement with our expectations both in regards to coverage and maximum gain. This data show that flat reflectarrays can give as well a defined footprint as a conventional antenna but without the complicated tooling and other drawbacks inherent for the latter.

Acknowledgment

This work was supported by the Research Department Institute of Engineering, Suranaree University of Technology, Thailand.

References

[1] R.E. Munson, H.A. Haddad, and J.W. Hanlen, "Microstrip reflectarray for satellite communications and RCS enhancement or reduction," U.S. patent 4 684 952, 1987.

[2] D.C. Chang and M.C. Huang, "Multiple-polarization microstrip reflectarray antenna with high efficiency and low cross-polarization," *IEEE Trans. on Antenna and Propag.*, Vol.43, No.8, 1995, pp. 829-834.

[3] J.A. Encinar, "Design of two-layer printed reflectarrays using patches of variable size," *IEEE Trans. on Antennas and Propag.*, Vol.49, 2001, pp.1403-1410.

[4] D. G. Kurup, M. Himdi, and A. Rydberg, "Design of an unequally spaced reflectarray," *IEEE Antennas and Wireless Propag. Letters*, Vol.2, 2003, pp.33-35.

[5] Peter F.M. Smulder, S. Khusial, and H.A.J. Herben, "A shaped reflector antenna for 60-GHz indoor wireless LAN access points," *IEEE Trans. on Verhicular Technology*, Vol. 50, No. 2, 2001, pp. 584-591.

[6] P. Krachodnok and R. Wongsan, "Design of microstrip reflectarray antenna using backscattering technique," *ITC-CSCC 2006 Conference Proceedings*, Thailand, Vol. 3, 2006, pp. 513-516.

[7] D.M. Pozar, S.D. Targonski, and R. Pokuls, "A shaped-beam microstrip patch reflectarray," *IEEE Trans. on Antenna and Propag.*, Vol.47, Issue 7, 1999, pp. 1167-1173.

[8] Kin-Lu Wong, *Compact and Broadband Microstrip Antenna*, John Wiley & Sons: New York, 2002, pp.22-86.

[9] J. Huang, Analysis of a microstrip reflectarray antenna for microspacecraft applications, The Telecommunications and Data Acquisition Progress Report 42-120, 1995, pp. 153-173.

[10] D.M. Pozar, S.D. Targonski, and H.D. Syrigos "Design of millimeter wave microstrip reflectarray," *IEEE Trans. on Antenna and Propagation*, Vol.45, No.2, 1997, pp. 287-296.